

Pell Wavelet Optimization Method for Solving Time-Fractional Convection Diffusion Equations Arising in Science and Medicine

Yadollah Ordokhani^{1*}, Sedigheh Sabermahani¹ and Mohsen Razzaghi²

¹Department of Mathematics, Faculty of Mathematical Sciences, Alzahra University, Tehran, Iran

²Department of Mathematics and Statistics, Mississippi State University, United States of America

Keywords:

Pell wavelets,
Time-fractional convection
diffusion equations,
Optimization solution

AMS Subject Classification (2020):

26A33; 35R11

Article History:

Received: 10 March 2024

Accepted: 29 July 2024

Abstract

Here, we present a composition method for solving time-fractional convection-diffusion equations (TF-CDEs). The main aims of the technique are to use Pell wavelets and convert the considered problem into fractional partial integro-differential equations, utilizing the Riemann-Liouville fractional integration (RL). For this approach, we consider Pell wavelets as an efficient tool to develop the method. We compute the RL pseudo-operational matrix for these functions. Taking RL for the considered problem and using the properties of RL, with the help of a pseudo-operational matrix and optimization scheme, we present the framework of the suggested scheme. Moreover, for approximate results, we evaluate the upper bound of errors. As a result, we apply the method by solving some numerical samples. Our approximate results illustrate that the computational scheme is powerful and applicable to solve the mentioned problems, and we can implement this to solve different kinds of fractional problems.

© 2024 University of Kashan Press. All rights reserved.

1 Introduction

In recent decades, with the expansion of science and the introduction of fractional calculus, fractional operators have been used widely to model various phenomena in science and mathematics because they provide new interpretations for classical models, as well as enabling alternatives in the formulation of phenomena models, whether they come from physics, chemistry, biology, or engineering [1–4]. The computational complexity in obtaining the analytical solution of some

*Corresponding author

E-mail addresses: ordokhani@alzahra.ac.ir (Y. Ordokhani), s.saber@alzahra.ac.ir (S. Sabermahani),

razzaghi@math.msstate.edu (M. Razzaghi)

Academic Editor: Abbas Saadatmandi

fractional problems caused the researchers to present various numerical methods according to the conditions and physics of the problem. For example, the authors proposed the fractional linear multi-step method for solving a class of fractional delay differential equations [5]. An operational matrix was designed to find the approximate solution of distributed order fractional differential equation [6].

Also, the effect of Caputo fractional derivative on polynomiography was studied in [7]. At the same time, convection-diffusion equations (CDEs) are a combination of the diffusion equation and convection, and describe some phenomena in which particles, electricity, and other physical quantities are transmitted in a physical structure through two methods; diffusion and convection [8–10].

Here, we aim to propose a hybrid computational method based on Pell wavelets and an optimization technique for TF-CDEs. We consider TF-CDE as follows [11]:

$${}_c D_t^\alpha \mathfrak{G}(x, t) + b(x)\mathfrak{G}_x(x, t) + c(x)\mathfrak{G}_{xx}(x, t) = g(x, t), \quad (1)$$

subject to

$$\mathfrak{G}(x, 0) = \mu(x),$$

and

$$\mathfrak{G}(0, t) = \eta_0(t), \quad \mathfrak{G}(1, t) = \eta_1(t),$$

for $(x, t) \in [0, 1] \times (0, 1]$, in which $b(x), c(x)$ are continuous functions, and $0 < \alpha \leq 1$. In this problem, Caputo fractional derivative is used, which is defined in [12].

For investigation, we utilize the main keyword, mentioned below, for searching in the Scopus database: (TITLE (diffusion AND equation) AND TITLE (convection) AND TITLE (fractional) AND TITLE (time)).

1.1 Existence and uniqueness solution

To study in existence and unique solution of this set of equations, some research existed. Hendy and Zaky [13] investigated existence, considered a class of TF-CDEs, and established the uniqueness and regularity properties of a weak solution. Also, Sun et al. [14] proved the existence, and uniqueness of the solution of using the fixed point theorem.

1.2 Applications

By applying the mentioned query in Scopus, the plot of the subject area of the problem is shown in Figure 1. Due to this figure, we can see that the most common use of this problem is in mathematics and engineering.

Convection diffusion equations (CDEs) are a combination of the diffusion equation and convection, and describe some natural events that electricity, particles, and some physical quantities are supplied in a physical structure through two methods; diffusion and convection [15]. Additionally, with the introduction and expansion of fractional calculus, fractional-order CDEs also appeared in the modeling of some phenomena to describe their behavior more accurately in engineering, physics, chemistry, and medicine. For instance, these types of equations have appeared in the modeling of mass transfer [16], gas transfer via heterogeneous soil and gas reservoirs [17], image processing [18], cholera spatial dynamics [19], continuous intestinal absorption model [20], gas desorption via a homogeneous membrane by Kalman filtering [21], chemical reactions [22], environmental science [23], liquid or pollutant transfer in heat conduction, and complex media [24], and global weather production in special case [25].

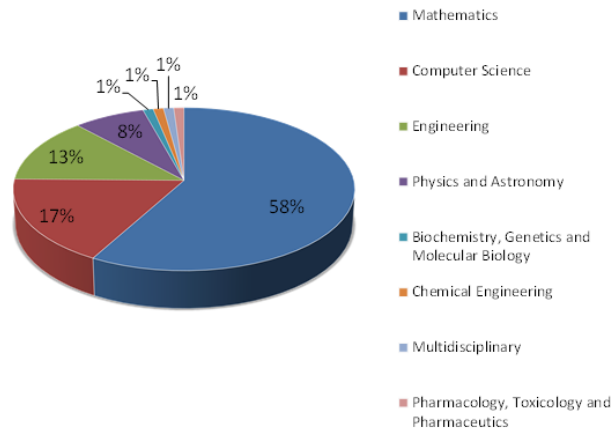


Figure 1: The subject area of the considered problems in Scopus.

1.3 Numerical studies

According to the considered keyword, the trend of annual published documents in Scopus is plotted in Figure 2. This data was collected on 16th May 2022. The existence and uniqueness

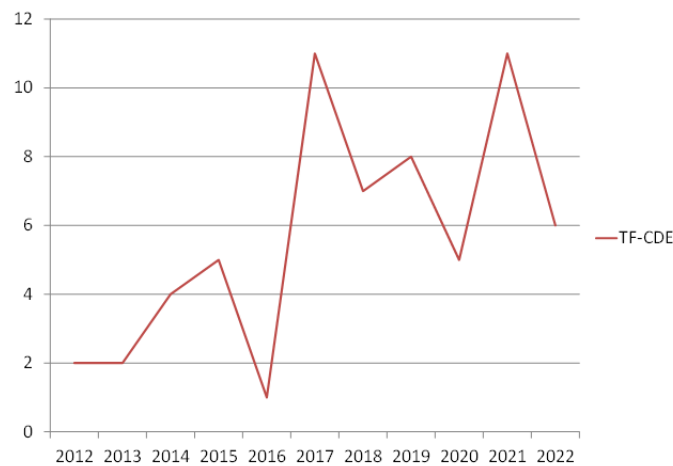


Figure 2: The trend of annual published documents in Scopus.

of the weak solution of space TF-CDE were investigated in [26]. The authors in [27] studied the existence, uniqueness, and regularity of the solution of TF-CDE. The stability and convergence of the different methods for the mentioned problems were perused in [28]. The convergence analysis of the shifted Chebyshev collocation of the fourth kind to solving the mentioned equation was investigated in [29].

Solution of TF-CDE has been investigated by some researchers and numerical techniques in this regard. For example, Sokhanvar et al. [30] presented a numerical scheme via Legendre multiwavelets to find a solution for multi-term fractional time-space CDEs. Two-dimensional TF-CDE was solved using Meshless simulation [31]. Authors [32] proposed a spectral method to solve the mentioned problems. Generalized polynomials were implemented to solve a class

of TF-CDEs [33]. Authors [34] studied a computational method via Jacobi polynomials. Lubo and Duressa [35] proposed a method based on the finite element method to solve the delay reaction-diffusion equation.

On the other hand, wavelets are effective and efficient tools to solve various kinds of problems with smooth or non-smooth solutions. Among of wavelet functions used to solve problems are Bernoulli wavelets [36], Fibonacci wavelets [37], Touchard wavelets [38], Taylor wavelets [39], and so on.

Finally, due to the efficiency of wavelet functions and the above discussion, we present a new computational technique by Pell wavelets. Due to the framework of the present method and RL pseudo-operational matrix, with an optimization scheme, we compute more accurate approximate solutions in comparing with some existing methods. Actually, the main aim of this manuscript is to transform the time-fractional diffusion equations into the fractional partial integro-differential equation by implementing the properties of the Caputo fractional derivative and the Riemann-Liouville integral. To do this, we proposed a new Riemann-Liouville pseudo-operational matrix for Pell wavelets. In the procedure of the matrix, we used the properties of the Riemann-Liouville integral, and the accuracy of this matrix affects the accuracy of the method directly. Moreover, applying an optimization method to derive the unknown coefficients affects the accuracy of the method, too.

1.4 Paper's structure

The study is structured as follows: Section 2 deals with recalling Pell polynomials, and wavelets and their properties. Section 3 provides a new RL pseudo-operational matrix applying characteristic functions. Section 4 presents the description of the suggested method. Section 5 proposes a discussion on error estimation. Section 6 provides some approximated experiments to illustrate the accuracy and effectiveness of the developed technique. Finally, Section 7 includes the conclusions of this manuscript.

2 Pell wavelets and their properties

Here, we recall the Pell polynomial and wavelet features.

2.1 Pell polynomials

Pell polynomials are defined as the following recurrence relation [40]

$$\begin{cases} \mathfrak{P}_m(t) = 2t\mathfrak{P}_{m-1}(t) + \mathfrak{P}_{m-2}(t), \\ \mathfrak{P}_0(t) = 0, \\ \mathfrak{P}_1(t) = 1, \quad m \geq 2. \end{cases} \quad (2)$$

These polynomials can be rewritten in the following form [41]

$$\mathfrak{P}_m(t) = \sum_{n=0}^{\lfloor \frac{m-1}{2} \rfloor} \binom{m-n-1}{n} (2t)^{m-2n-1}, \quad (3)$$

with the following property for $m \geq 0$ [42]

$$t^m = \left(\frac{1}{2}\right)^m \sum_{r=0}^{\lfloor \frac{m}{2} \rfloor} (-1)^r \binom{m}{r} \frac{m-2r+1}{m-r+1} \mathfrak{P}_{m+1-2r}(t). \quad (4)$$

Lemma 2.1. For the Pell polynomials, we have the following feature [43]

$$\int_0^1 \mathfrak{P}_m(t) \mathfrak{P}_{m'}(t) dt = \sum_{n=0}^{\lfloor \frac{m-1}{2} \rfloor} \sum_{n'=0}^{\lfloor \frac{m'-1}{2} \rfloor} \binom{m-n-1}{n} \binom{m'-n'-1}{n'} \frac{2^{m+m'-2n-2n'-2}}{m+m'-2n-2n'-1}. \quad (5)$$

2.2 Wavelet functions

Here, we consider the Pell wavelets in the following form [43]

$$\psi_{n,m}(t) = \begin{cases} 2^{\frac{k-1}{2}} \tilde{\mathfrak{P}}_m(2^{k-1}t - \tilde{n}), & t \in [\frac{\tilde{n}}{2^{k-1}}, \frac{\tilde{n}+1}{2^{k-1}}), \\ 0, & \text{otherwise,} \end{cases} \quad (6)$$

in which, $m = 1, 2, \dots, M$, $n = 1, 2, \dots, 2^{k-1}$, $\tilde{\mathfrak{P}}_m(t) = \frac{1}{\sqrt{\omega_m}} \mathfrak{P}_m(t)$, and ω_m is derived using Equation (5).

In this part, we can approximate a square-integrable function $u(x, t)$ utilizing Pell wavelets in the following formula:

$$\begin{aligned} u(x, t) &\approx \sum_{n=1}^{2^{k-1}} \sum_{m=1}^M \sum_{\tilde{n}=1}^{2^{\tilde{k}-1}} \sum_{\tilde{m}=1}^{\tilde{M}} u_{n,m,\tilde{n},\tilde{m}} \psi_{n,m}(x) \psi_{\tilde{n},\tilde{m}}(t) \\ &= (\Psi_k^M(x))^T U \Psi_{\tilde{k}}^{\tilde{M}}(t), \end{aligned} \quad (7)$$

in which

$$\begin{aligned} \Psi_k^M(x) &= [\psi_{1,1}(x), \dots, \psi_{1,M}(x), \dots, \psi_{2^{k-1},1}(x), \dots, \psi_{2^{k-1},M}(x)]^T, \\ \Psi_{\tilde{k}}^{\tilde{M}}(t) &= [\psi_{1,1}(t), \dots, \psi_{1,\tilde{M}}(t), \dots, \psi_{2^{\tilde{k}-1},1}(t), \dots, \psi_{2^{\tilde{k}-1},\tilde{M}}(t)]^T, \end{aligned}$$

and we calculate the unknown matrix U via the following formula:

$$U = \frac{\langle \Psi_k^M(x), \langle u(x, t), \Psi_{\tilde{k}}^{\tilde{M}}(t) \rangle \rangle}{\langle \Psi_k^M(x), \Psi_k^M(x) \rangle \langle \Psi_{\tilde{k}}^{\tilde{M}}(t), \Psi_{\tilde{k}}^{\tilde{M}}(t) \rangle}.$$

3 RL pseudo-operational matrix

RL integration is one of the most applicable concepts in fractional calculus. To find the definition and some existing properties, Refs. [12, 44] are suitable.

Here, we describe the method to compute a fractional pseudo-operational matrix for Pell wavelets. Suppose that

$$\mathfrak{J}_t^\alpha \Psi_k^M(t) \approx t^\alpha \Lambda(\alpha) \Psi_k^M(t), \quad (8)$$

where $t^\alpha \Lambda(\alpha) \triangleq \Lambda(\alpha, t)$ denotes the RL pseudo-operational matrix. The strategy to calculate the components of the mentioned matrix is discussed below.

Theorem 3.1. Suppose that $\psi_{n,m}(t)$ is the component of the Pell wavelets vector. Then, the RL of the component of order $n - 1 \leq \alpha < n$ is obtained as:

$$\mathfrak{J}_t^\alpha \psi_{n,m}(t) \approx t^\alpha \sum_{i=1}^{2^{k-1}} \sum_{j=1}^M \xi_{i,j}^{m,n} \psi_{i,j}(t), \quad (9)$$

where

$$\xi_{i,j}^{m,n} = \frac{2^{\frac{k-1}{2}}}{\sqrt{\omega_m}} \sum_{s=0}^{\lfloor \frac{m-1}{2} \rfloor} \sum_{r=0}^{m-2s-1} \binom{m-s-1}{s} \binom{m-2s-1}{r} 2^{kr} (2-2n)^{m-2s-1-r} a_{i,j}.$$

Proof. Due to the definition of $\psi_{n,m}(t)$ in Equation (6), we can rewrite this relation as:

$$\psi_{n,m}(t) = 2^{\frac{k-1}{2}} \tilde{\mathfrak{P}}_m(2^{k-1}t - \tilde{n}) \chi_{[\frac{\tilde{n}}{2^{k-1}}, \frac{\tilde{n}+1}{2^{k-1}})}(t), \quad (10)$$

in which $\chi_{[a,b)}(t)$ is the characteristic function. Next, according to Equation (3) and the afore-said representation, the following expression is derived

$$\begin{aligned} \mathfrak{J}_t^\alpha \psi_{n,m}(t) &= \mathfrak{J}_t^\alpha \left(2^{\frac{k-1}{2}} \tilde{\mathfrak{P}}_m(2^{k-1}t - \tilde{n}) \chi_{[\frac{\tilde{n}}{2^{k-1}}, \frac{\tilde{n}+1}{2^{k-1}})}(t) \right) \quad (11) \\ &= \frac{2^{\frac{k-1}{2}}}{\sqrt{\omega_m}} \mathfrak{J}_t^\alpha \left(\sum_{s=0}^{\lfloor \frac{m-1}{2} \rfloor} \binom{m-s-1}{s} (2^k t - 2n + 2)^{m-2s-1} \chi_{[\frac{n-1}{2^{k-1}}, \frac{n}{2^{k-1}})}(t) \right) \\ &= \frac{2^{\frac{k-1}{2}}}{\sqrt{\omega_m}} \sum_{s=0}^{\lfloor \frac{m-1}{2} \rfloor} \sum_{r=0}^{m-2s-1} \binom{m-s-1}{s} \binom{m-2s-1}{r} 2^{kr} (2-2n)^{m-2s-1-r} \\ &\times \mathfrak{J}_t^\alpha \left(t^r \chi_{[\frac{n-1}{2^{k-1}}, \frac{n}{2^{k-1}})}(t) \right) \\ &= \frac{2^{\frac{k-1}{2}}}{\sqrt{\omega_m}} \sum_{s=0}^{\lfloor \frac{m-1}{2} \rfloor} \sum_{r=0}^{m-2s-1} \binom{m-s-1}{s} \binom{m-2s-1}{r} 2^{kr} (2-2n)^{m-2s-1-r} \theta_r(t), \end{aligned}$$

we approximate $\theta_r(t)$ using the Pell wavelets as:

$$\begin{aligned} \theta_r(t) &= \mathfrak{J}_t^\alpha \left(t^r \chi_{[\frac{n-1}{2^{k-1}}, \frac{n}{2^{k-1}})}(t) \right) \quad (12) \\ &\approx t^\alpha \sum_{i=1}^{2^{k-1}} \sum_{j=1}^M a_{i,j} \psi_{i,j}(t). \end{aligned}$$

Then, we insert the above equation in Equation (11), so we get

$$\mathfrak{J}_t^\alpha \psi_{n,m}(t) \approx t^\alpha \sum_{i=1}^{2^{k-1}} \sum_{j=1}^M \xi_{i,j}^{m,n} \psi_{i,j}(t),$$

where

$$\xi_{i,j}^{m,n} = \frac{2^{\frac{k-1}{2}}}{\sqrt{\omega_m}} \sum_{s=0}^{\lfloor \frac{m-1}{2} \rfloor} \sum_{r=0}^{m-2s-1} \binom{m-s-1}{s} \binom{m-2s-1}{r} 2^{kr} (2-2n)^{m-2s-1-r} a_{i,j}.$$

■

4 Construction of algorithm

In this portion, we establish our required relations for computation of solution of Equation (1). To this aim, we consider Equation (1). For the first step, with respect to t (\mathfrak{J}_t^α), we apply RL integration in order α in the both sides of equation, then we get

$$\mathfrak{G}(x, t) + b(x)\mathfrak{J}_t^\alpha (\mathfrak{G}_x(x, t)) + c(x)\mathfrak{J}_t^\alpha (\mathfrak{G}_{xx}(x, t)) = \mathfrak{J}_t^\alpha (g(x, t)) + \mathfrak{G}(x, 0), \quad (13)$$

in the next step, we approximate $\mathfrak{G}_{xx}(x, t)$, which has the highest order of derivative using the Pell wavelets as:

$$\mathfrak{G}_{xx}(x, t) \approx \Psi_k^{MT}(x)U\Psi_k^{\tilde{M}}(t), \quad (14)$$

and $U = [u_{n,m}]$, $n = 1, 2, \dots, 2^{k-1}$, $m = 1, 2, \dots, M$. By taking integral of order 1 with respect to x in Equation (14), and implement the boundary conditions, the following relation is achieved.

$$\mathfrak{G}_x(x, t) \approx \Psi_k^{MT}(x)\Lambda(1, x)^T U\Psi_k^{\tilde{M}}(t) + \mathfrak{G}_x(0, t), \quad (15)$$

and, $\mathfrak{G}_x(0, t)$ is unknown function. Similarly, we achieve

$$\begin{aligned} \mathfrak{G}(x, t) &\approx \Psi_k^{MT}(x)\Lambda(2, x)^T U\Psi_k^{\tilde{M}}(t) + x\mathfrak{G}_x(0, t) + \mathfrak{G}(0, t) \\ &= \Psi_k^{MT}(x)\Lambda(2, x)^T U\Psi_k^{\tilde{M}}(t) + x\mathfrak{G}_x(0, t) + \eta_0(t). \end{aligned} \quad (16)$$

Now, to compute the unknown function $\mathfrak{G}_x(0, t)$, we take the integral from Equation (15) on the interval $[0, 1]$, thus we get

$$\mathfrak{G}_x(0, t) \approx \eta_1(t) - \eta_0(t) - \left[\int_0^1 \Psi_k^{MT}(x)\Lambda(1, x)^T dx \right] U\Psi_k^{\tilde{M}}(t). \quad (17)$$

In the following, due to Equation (13) and Equations (14)-(17), we take the RL fractional integration of order α , from Equations (14)-(16). Thus, the following relation are achieved.

$$\mathfrak{J}_t^\alpha (\mathfrak{G}_{xx}(x, t)) \approx \Psi_k^{MT}(x)U\Lambda(\alpha, t)\Psi_k^{\tilde{M}}(t), \quad (18)$$

$$\begin{aligned} \mathfrak{J}_t^\alpha (\mathfrak{G}_x(x, t)) &\approx \Psi_k^{MT}(x)\Lambda(1, x)^T U\Lambda(\alpha, t)\Psi_k^{\tilde{M}}(t) + \mathfrak{J}_t^\alpha (\mathfrak{G}_x(0, t)) \\ &\approx \Psi_k^{MT}(x)\Lambda(1, x)^T U\Lambda(\alpha, t)\Psi_k^{\tilde{M}}(t) + \left(\mathfrak{J}_t^\alpha (\eta_1(t)) - \mathfrak{J}_t^\alpha (\eta_0(t)) \right. \\ &\quad \left. - \left[\int_0^1 \Psi_k^{MT}(x)\Lambda(1, x)^T dx \right] U\Lambda(\alpha, t)\Psi_k^{\tilde{M}}(t) \right), \end{aligned} \quad (19)$$

$$\begin{aligned} \mathfrak{J}_t^\alpha (\mathfrak{G}(x, t)) &\approx \Psi_k^{MT}(x)\Lambda(2, x)^T U\Lambda(\alpha, t)\Psi_k^{\tilde{M}}(t) + x\mathfrak{J}_t^\alpha (\mathfrak{G}_x(0, t)) + \mathfrak{J}_t^\alpha (\eta_0(t)) \\ &\approx \Psi_k^{MT}(x)\Lambda(2, x)^T U\Lambda(\alpha, t)\Psi_k^{\tilde{M}}(t) + x\left(\mathfrak{J}_t^\alpha (\eta_1(t)) - \mathfrak{J}_t^\alpha (\eta_0(t)) \right. \\ &\quad \left. - \left[\int_0^1 \Psi_k^{MT}(x)\Lambda(1, x)^T dx \right] U\Lambda(\alpha, t)\Psi_k^{\tilde{M}}(t) \right) + \mathfrak{J}_t^\alpha (\eta_0(t)). \end{aligned} \quad (20)$$

Consequently, inserting Equations (14)-(20) in Equation (13), we have

$$\begin{aligned} \mathfrak{R}(x, t) \triangleq & \Psi_k^{MT}(x)\Lambda(2, x)^T U \Psi_k^{\tilde{M}}(t) + x \left(\eta_1(t) - \eta_0(t) - \left[\int_0^1 \Psi_k^{MT}(x)\Lambda(1, x)^T dx \right] U \Psi_k^{\tilde{M}}(t) \right) \\ & + \eta_0(t) + b(x) \left(\Psi_k^{MT}(x)\Lambda(1, x)^T U \Lambda(\alpha, t) \Psi_k^{\tilde{M}}(t) + \left[\mathfrak{I}_t^\alpha (\eta_1(t)) - \mathfrak{I}_t^\alpha (\eta_0(t)) \right. \right. \\ & - \left. \left. \left[\int_0^1 \Psi_k^{MT}(x)\Lambda(1, x)^T dx \right] U \Lambda(\alpha, t) \Psi_k^{\tilde{M}}(t) \right] \right) + c(x) \left(\Psi_k^{MT}(x) U \Lambda(\alpha, t) \Psi_k^{\tilde{M}}(t) \right) \\ & - \mathfrak{I}_t^\alpha (g(x, t)) + \mu(x). \end{aligned} \tag{21}$$

Finally, we can find the unknown matrix U , equivalently, in the optimization problem

$$\mathfrak{J} = \int_0^1 \int_0^1 \mathfrak{R}^2(x, t) dx dt, \tag{22}$$

for the extremum of \mathfrak{J} , the necessary conditions are computed as:

$$\frac{\partial \mathfrak{J}}{\partial U} = 0.$$

We solve the aforesaid system via mathematica software packages. After calculating U , we obtain the numerical solution through Equation (16).

5 Error analysis

In this section, the approximation error bound is proposed. The Sobolev norm concept is presented in [45]. We consider this norm in $\Omega = (a, b)^s \in \mathbb{R}, s = 2, 3$. Moreover, the following seminorms are required to achieve the aim [45].

$$|u|_{H^{\nu;M}(a,b)} = \left(\sum_{i=\min(\nu, M+1)}^{\nu} \|u^{(i)}\|_{L^2(a,b)}^2 \right)^{\frac{1}{2}}, \tag{23}$$

and

$$|u|_{H^{r,\nu;M,N}(a,b)} = \left(\sum_{i=\min(\nu, M+1)}^{\nu} N^{2r-2i} \|u^{(i)}\|_{L^2(a,b)}^2 \right)^{\frac{1}{2}}, \tag{24}$$

where, $u \in H^\nu(a, b), 0 \leq r \leq \nu, M \geq 1$ and $N \geq 1$. Also, according to the mentioned seminorms, we have

$$|u|_{H^{r,\nu;M,N}(a,b)} = N^{r-\nu} \|u^{(\nu)}\|_{L^2(a,b)}.$$

Remark 1. The following relation named Sobolev inequality, is established [46]

$$\|u\|_{L^\infty(a,b)} \leq \left[\frac{1}{b-a} + 2 \right]^{\frac{1}{2}} \|u\|_{L^2(a,b)}^{\frac{1}{2}} \|u\|_{H^1(a,b)}^{\frac{1}{2}}. \tag{25}$$

Lemma 5.1. Suppose that $u \in H^\nu(0, 1), \nu \geq 1$, then we have [47]

$$\tilde{u} \approx \sum_{n=1}^{2^{k-1}} \sum_{\tilde{m}=1}^{\tilde{M}} c_{n,\tilde{m}} \psi_{n,\tilde{m}}(t),$$

where, \tilde{u} is the best approximation of u , therefore

$$\|u - \tilde{u}\|_{L^2(0,1)} \leq \varrho \tilde{M}^{-\nu} |u|_{H^{0,\nu;\tilde{M},2^{k-1}}(0,1)},$$

also, we get

$$\|u - \tilde{u}\|_{H^r(0,1)} \leq \varrho \tilde{M}^{\sigma(r)-\nu} |u|_{H^{r,\nu;\tilde{M},2^{k-1}}(0,1)},$$

where $1 \leq r \leq \nu$, ϱ depends on ν , and

$$\sigma(r) = \begin{cases} 2r - \frac{1}{2}, & r > 0, \\ 0, & r = 0. \end{cases}$$

Lemma 5.2. *If the hypothesis of the above lemma holds, we get:*

$$\|u - \tilde{u}\|_{L^\infty(0,1)} \leq \sqrt{3} \varrho \tilde{M}^{\frac{3}{4}-\nu} 2^{\frac{k-1}{2}} |u|_{H^{0,\nu;\tilde{M},2^{k-1}}(0,1)}. \tag{26}$$

Proof. Due to Remark 1, and Lemma 5.2, we obtain:

$$\begin{aligned} \|u - \tilde{u}\|_{L^\infty(0,1)} &\leq \sqrt{3} \|u - \tilde{u}\|_{L^2(0,1)}^{\frac{1}{2}} \|u - \tilde{u}\|_{H^1(0,1)}^{\frac{1}{2}} \\ &\leq \sqrt{3} \varrho \tilde{M}^{\frac{3}{4}-\nu} |u|_{H^{1,\nu;\tilde{M},2^{k-1}}(0,1)}^{\frac{1}{2}} |u|_{H^{0,\nu;\tilde{M},2^{k-1}}(0,1)}^{\frac{1}{2}} \\ &= \sqrt{3} \varrho \tilde{M}^{\frac{3}{4}-\nu} \left(\sum_{\min(\nu, \tilde{M}+1)}^{\nu} (2^{k-1})^{2-2i} \|u^{(i)}\|_{L^2(0,1)}^2 \right)^{\frac{1}{4}} \\ &\quad \times \left(\sum_{\min(\nu, \tilde{M}+1)}^{\nu} (2^{k-1})^{-2i} \|u^{(i)}\|_{L^2(0,1)}^2 \right)^{\frac{1}{4}} \\ &= \sqrt{3} \varrho \tilde{M}^{\frac{3}{4}-\nu} 2^{\frac{k-1}{2}} \left(\sum_{\min(\nu, \tilde{M}+1)}^{\nu} (2^{k-1})^{-2i} \|u^{(i)}\|_{L^2(0,1)}^2 \right)^{\frac{1}{2}} \\ &= \sqrt{3} \varrho \tilde{M}^{\frac{3}{4}-\nu} 2^{\frac{k-1}{2}} |u|_{H^{0,\nu;\tilde{M},2^{k-1}}(0,1)}. \end{aligned}$$

Then, the proof is complete. ■

Theorem 5.3. *Let $\hat{u}_{\tilde{M}}$ is the approximation of $\mathfrak{U}_{\tilde{M}}$ where*

$$\mathfrak{U}_{\tilde{M}}(x, t) = \sum_{n=1}^{2^{k-1}} \sum_{\hat{m}=1}^{\infty} a_{n,\hat{m},\tilde{M}} \psi_{n,\tilde{M}}(x) \psi_{n,\hat{m}}(t),$$

and

$$\hat{u}_{\tilde{M}}(x, t) = \sum_{n=1}^{2^{k-1}} \sum_{\hat{m}=1}^{\tilde{M}} a_{n,\hat{m},\tilde{M}} \psi_{n,\tilde{M}}(x) \psi_{n,\hat{m}}(t),$$

so, the following relation is derived.

$$\|\mathfrak{U}_{\tilde{M}} - \hat{u}_{\tilde{M}}\|_{L^\infty(0,1)} \leq \sqrt{3} \varrho \mathfrak{M}_{\tilde{M}} \tilde{M}^{\frac{3}{4}-\nu} 2^{\frac{k-1}{2}} |u|_{H^{0,\nu;\tilde{M},2^{k-1}}(0,1)}, \tag{27}$$

where, $\mathfrak{M}_{\tilde{M}} = \sup_{x \in [0,1]} \left| \sum_{n=1}^{2^{k-1}} \psi_{n,\tilde{M}}(x) \right|$.

Proof. Due to the hypotheses, Lemma 5.2, and $\Lambda = [0, 1] \times [0, 1]$, we achieve

$$\begin{aligned} & \|\mathfrak{U}_{\tilde{M}} - \hat{u}_{\tilde{M}}\|_{L^\infty(0,1)} \\ &= \sup_{(x,t) \in \Lambda} \left| \sum_{n=1}^{2^{k-1}} \sum_{\hat{m}=1}^{\infty} a_{n,\hat{m},\tilde{M}} \psi_{n,\tilde{M}}(x) \psi_{n,\hat{m}}(t) - \sum_{n=1}^{2^{k-1}} \sum_{\hat{m}=1}^{\tilde{M}} a_{n,\hat{m},\tilde{M}} \psi_{n,\tilde{M}}(x) \psi_{n,\hat{m}}(t) \right| \\ &= \sup_{(x,t) \in \Lambda} \left| \left(\sum_{n=1}^{2^{k-1}} \sum_{\hat{m}=1}^{\infty} a_{n,\hat{m},\tilde{M}} \psi_{n,\tilde{M}}(x) \psi_{n,\hat{m}}(t) - \sum_{n=1}^{2^{k-1}} \sum_{\hat{m}=1}^{\tilde{M}} a_{n,\hat{m},\tilde{M}} \psi_{n,\tilde{M}}(x) \psi_{n,\hat{m}}(t) \right) \left(\sum_{n=1}^{2^{k-1}} \psi_{n,\tilde{M}}(x) \right) \right| \\ &\leq \sup_{t \in [0,1]} \left| \sum_{n=1}^{2^{k-1}} \sum_{\hat{m}=1}^{\infty} a_{n,\hat{m},\tilde{M}} \psi_{n,\tilde{M}}(x) \psi_{n,\hat{m}}(t) - \sum_{n=1}^{2^{k-1}} \sum_{\hat{m}=1}^{\tilde{M}} a_{n,\hat{m},\tilde{M}} \psi_{n,\tilde{M}}(x) \psi_{n,\hat{m}}(t) \right| \sup_{x \in [0,1]} \left| \sum_{n=1}^{2^{k-1}} \psi_{n,\tilde{M}}(x) \right| \\ &= \mathfrak{M}_{\tilde{M}} \left\| \sum_{n=1}^{2^{k-1}} \sum_{\hat{m}=1}^{\infty} a_{n,\hat{m},\tilde{M}} \psi_{n,\tilde{M}}(x) \psi_{n,\hat{m}}(t) - \sum_{n=1}^{2^{k-1}} \sum_{\hat{m}=1}^{\tilde{M}} a_{n,\hat{m},\tilde{M}} \psi_{n,\tilde{M}}(x) \psi_{n,\hat{m}}(t) \right\|_{L^\infty(0,1)} \\ &\leq \sqrt{3} \varrho \mathfrak{M}_{\tilde{M}} \hat{M}^{\frac{3}{4}-\nu} 2^{\frac{k-1}{2}} |u|_{H^{0,\nu;\tilde{M},2^{k-1}}(0,1)}. \end{aligned}$$

where, $\mathfrak{M}_{\tilde{M}} = \sup_{x \in [0,1]} \left| \sum_{n=1}^{2^{k-1}} \psi_{n,\tilde{M}}(x) \right|$. ■

Remark 2. According to the above theorem, we can consider $\hat{u}_{\tilde{M}}$ is the approximation of $\mathfrak{U}_{\tilde{M}}$, where

$$\mathfrak{U}_{\tilde{M}}(x, t) = \sum_{n=1}^{2^{k-1}} \sum_{\hat{m}=1}^{\infty} a_{n,\hat{m},\tilde{M}} \psi_{n,\tilde{M}}(x) \psi_{n,\hat{m}}(t),$$

and

$$\hat{u}_{\tilde{M}}(x, t) = \sum_{n=1}^{2^{k-1}} \sum_{\hat{m}=1}^{\tilde{M}} a_{n,\hat{m},\tilde{M}} \psi_{n,\tilde{M}}(x) \psi_{n,\hat{m}}(t),$$

then, we have

$$\|\mathfrak{U}_{\tilde{M}} - \hat{u}_{\tilde{M}}\|_{L^\infty(0,1)} \leq \sqrt{3} \varrho \mathfrak{M}_{\tilde{M}} \tilde{M}^{\frac{3}{4}-\nu} 2^{\frac{k-1}{2}} |u|_{H^{0,\nu;\tilde{M},2^{k-1}}(0,1)}, \tag{28}$$

where, $\mathfrak{M}_{\tilde{M}} = \sup_{t \in [0,1]} \left| \sum_{n=1}^{2^{k-1}} \psi_{n,\tilde{M}}(t) \right|$.

Corollary 5.4. *Considering the above lemmas, theorem, and remark, and by considering $\hat{M}, \tilde{M} > \nu - 1, \nu \geq 1$, we conclude*

$$\|\mathfrak{U}_{\tilde{M}} - \hat{u}_{\tilde{M}}\|_{L^\infty(0,1)} \leq \sqrt{3} \varrho \mathfrak{M}_{\tilde{M}} \hat{M}^{\frac{3}{4}-\nu} (2^{\frac{k-1}{2}})^{\frac{1}{2}-\nu} \|\mathfrak{U}_{\tilde{M}}^{(\nu)}\|_{L^2(0,1)}, \tag{29}$$

and

$$\|\mathfrak{U}_{\tilde{M}} - \hat{u}_{\tilde{M}}\|_{L^\infty(0,1)} \leq \sqrt{3} \varrho \mathfrak{M}_{\tilde{M}} \tilde{M}^{\frac{3}{4}-\nu} (2^{\frac{k-1}{2}})^{\frac{1}{2}-\nu} \|\mathfrak{U}_{\tilde{M}}^{(\nu)}\|_{L^2(0,1)}. \tag{30}$$

Therefore, increasing the amount of \tilde{M}, \hat{M} and k , the above error bound tends to zero.

6 Test sample

Some samples are given to display the superiority and accuracy properties of the developed scheme.

Sample 1: The following TF-CDE is considered

$${}_c D_t^\alpha \mathfrak{G}(x, t) + x \mathfrak{G}_x(x, t) - \mathfrak{G}_{xx}(x, t) = g(x, t),$$

where

$$\mathfrak{G}(0, t) = \mathfrak{G}(1, t) = 0, \quad \mathfrak{G}(x, 0) = x^2 - x^3,$$

and

$$g(x, t) = \frac{2t^{2-\alpha}}{\Gamma(3-\alpha)}(x^2 - x^3) + (t^2 + 1)(2x^2 - 3x^3 + 6x - 2).$$

$\mathfrak{G}(x, t) = (x^2 - x^3)(t^2 + 1)$ is the analytic solution of this problem.

Using the present method, the absolute errors (AEs) for $\alpha = 1, 0.5$ with $k = \tilde{k} = 1, M = \tilde{M} = 3$ are displayed in Figure 3. Besides, the absolute errors with $k = \tilde{k} = 2, M = \tilde{M} = 3$ at $t = 0.2$ for some values of α are demonstrated in Figure 4.

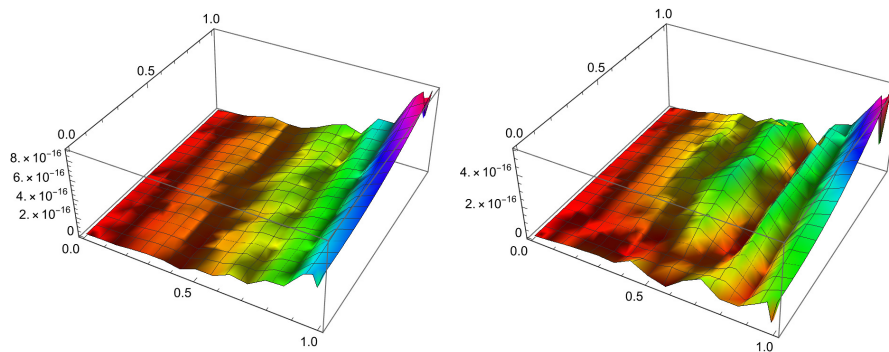


Figure 3: AE for Sample 1 with $k = \tilde{k} = 1, M = \tilde{M} = 3, \alpha = 0.5$ (left) and $\nu = 1$ (right).

Sample 2: The following TF-CDE is considered

$${}_c D_t^\alpha \mathfrak{G}(x, t) + \mathfrak{G}_x(x, t) - x \mathfrak{G}_{xx}(x, t) = g(x, t),$$

subject to

$$\mathfrak{G}(0, t) = (t^2 + 1)(1 - t), \quad \mathfrak{G}(1, t) = (t^2 + 1)(e - t), \quad \mathfrak{G}(x, 0) = e^x,$$

and

$$g(x, t) = \frac{2t^{2-\alpha}}{\gamma(3-\alpha)}e^x - \frac{t^{1-\alpha}}{\gamma(2-\alpha)} - \frac{6t^{3-\alpha}}{\gamma(4-\alpha)} + (t^2 + 1)(1 - x)e^x.$$

The exact solution for this sample is

$$\mathfrak{G}(x, t) = (t^2 + 1)(e^x - t).$$

We apply the developed scheme to solve this problem and the numerical results are proposed in Table 1, Figures 5 and 6. The comparison derived results of the proposed technique with the

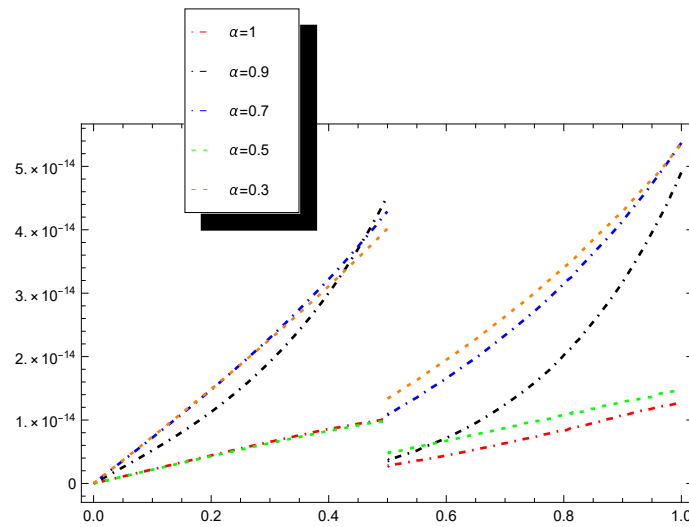


Figure 4: AE for Sample 1 with $k = \tilde{k} = 2, M = \tilde{M} = 3, t = 0.2$ and different values of α .

Table 1: AEs obtained by Tk-ChWs and our scheme for Sample 2.

(x, t)	$\alpha = 0.9$		$\alpha = 0.3$	
	Tk-ChWs ($k = 2, M = 6$)	Our method ($k = \tilde{k} = 1, M = \tilde{M} = 6$)	Tk-ChWs ($k = 2, M = 6$)	Our method ($k = \tilde{k} = 1, M = \tilde{M} = 6$)
(0.1, 0.1)	$2.5576 e^{-5}$	$1.4602 e^{-9}$	$7.7516 e^{-6}$	$1.8787 e^{-9}$
(0.2, 0.2)	$3.5050 e^{-5}$	$6.7131 e^{-9}$	$1.7024 e^{-5}$	$4.6047 e^{-9}$
(0.3, 0.3)	$3.3778 e^{-5}$	$1.9372 e^{-9}$	$2.4422 e^{-5}$	$5.2454 e^{-10}$
(0.4, 0.4)	$2.7183 e^{-5}$	$1.2652 e^{-9}$	$2.8796 e^{-5}$	$3.4321 e^{-9}$
(0.5, 0.5)	$2.0780 e^{-5}$	$1.6367 e^{-9}$	$3.0385 e^{-5}$	$1.4401 e^{-10}$
(0.6, 0.6)	$1.5150 e^{-5}$	$3.6819 e^{-9}$	$2.8824 e^{-5}$	$2.5257 e^{-9}$
(0.7, 0.7)	$1.0310 e^{-5}$	$4.5087 e^{-10}$	$2.4550 e^{-5}$	$1.7513 e^{-10}$
(0.8, 0.8)	$6.2760 e^{-6}$	$2.4375 e^{-9}$	$1.7352 e^{-5}$	$2.1079 e^{-9}$
(0.9, 0.9)	$2.9178 e^{-6}$	$1.3009 e^{-10}$	$9.5897 e^{-6}$	$2.2314 e^{-10}$

scheme based on the third kind Chebyshev wavelets (Tk-ChWs) [48] are reported in Table 1. This table shows that the suggested method is more accurate than the Tk-ChWs. Indeed, a small number of Pell wavelets is utilized to derive satisfactory results. Moreover, the exact and numerical solution for $k = 1, \tilde{k} = 2, M = 10, \tilde{M} = 6$ and $\alpha = 1$ are shown in Figure 5. Besides, the density of the exact and numerical solution over slice surface x for $k = 1, \tilde{k} = 2, M = 10, \tilde{M} = 6$ and $\alpha = 1$ are displayed in Figure 6.

Sample 3: We consider the following TF-CDE

$${}_c D_t^\alpha \mathfrak{G}(x, t) + x \mathfrak{G}_x(x, t) + \mathfrak{G}_{xx}(x, t) = g(x, t),$$

in which

$$\mathfrak{G}(0, t) = \frac{2\gamma(\alpha + 1)}{\gamma(2\alpha + 1)} t^{2\alpha}, \quad \mathfrak{G}(1, t) = 1 + \frac{2\gamma(\alpha + 1)}{\gamma(2\alpha + 1)}, \quad \mathfrak{G}(x, 0) = x^2,$$

and $g(x, t) = 2t^\alpha + 2x^2 + 2$. The exact solution of the sample is $\mathfrak{G}(x, t) = x^2 + \frac{2\gamma(\alpha+1)}{\gamma(2\alpha+1)} t^{2\alpha}$.

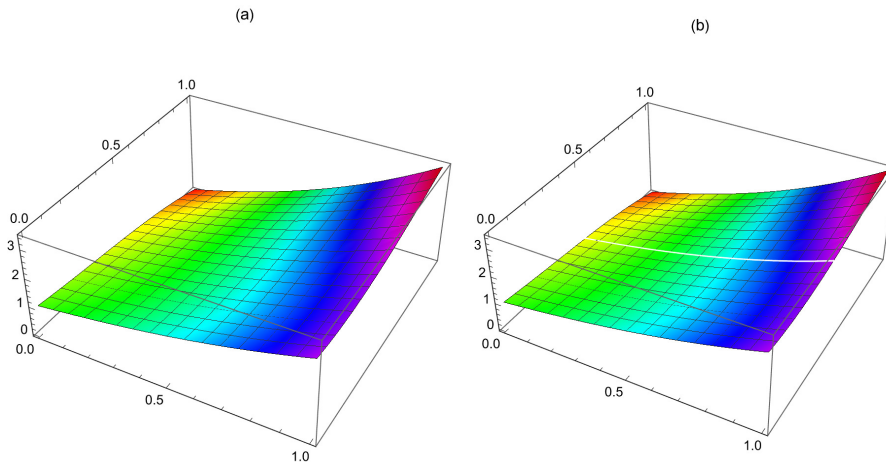


Figure 5: (a) The exact solution and (b) approximate solution with $k = 1, \tilde{k} = 2, M = 10, \tilde{M} = 6,$ and $\alpha = 1$ in Sample 2.

We implement the proposed technique to find the approximate solution of the considered sample. In Table 2, the comparison of the absolute errors of the Haar wavelet method [49], Sinc-Legendre method [11], and the developed scheme are listed. In this table, it's clear that the suggested scheme is more accurate than the mentioned methods. Additionally, AEs of the problem derived by the proposed scheme for $k = \tilde{k} = M = \tilde{M} = 2$ and $\alpha = 0.5, 0.3$ are plotted in Figure 7.

Table 2: Comparison of AEs obtained by the present and other schemes for $\alpha = 0.5$ in Sample 3.

(x, t)	Haar wavelet method ($m = 64$)	Sinc-Legendre wavelet method ($m = 25$)	Present method ($k = \tilde{k} = 1, M = \tilde{M} = 2$)
(0.1, 0.5)	$1.210 e^{-3}$	$6.462 e^{-6}$	$4.45511 e^{-18}$
(0.2, 0.5)	$1.259 e^{-3}$	$1.578 e^{-5}$	$7.17304 e^{-18}$
(0.3, 0.5)	$1.865 e^{-3}$	$2.272 e^{-5}$	$8.49590 e^{-18}$
(0.4, 0.5)	$7.412 e^{-3}$	$2.674 e^{-5}$	$8.76575 e^{-18}$
(0.5, 0.5)	$1.000 e^{-6}$	$2.759 e^{-5}$	$8.32471 e^{-18}$
(0.6, 0.5)	$7.460 e^{-3}$	$2.534 e^{-4}$	$7.51485 e^{-18}$
(0.7, 0.5)	$1.724 e^{-3}$	$2.035 e^{-4}$	$6.67827 e^{-18}$
(0.8, 0.5)	$4.990 e^{-3}$	$1.320 e^{-4}$	$6.15705 e^{-18}$
(0.9, 0.5)	$1.678 e^{-2}$	$4.653 e^{-6}$	$6.29329 e^{-18}$

Sample 4: We consider the following TF-CDE

$${}_c D_t^\alpha \mathfrak{G}(x, t) - \mathfrak{G}_{xx}(x, t) + \mathfrak{G}_x(x, t) = g(x, t),$$

in which

$$\mathfrak{G}(0, t) = \mathfrak{G}(1, t) = \mathfrak{G}(x, 0) = 0,$$

and $g(x, t) = \frac{\Gamma(4+\alpha)t^3}{6} \sin(\pi x) + \pi^2 t^{3+\alpha} \sin(\pi x) + \pi t^{3+\alpha} \cos(\pi x)$. The analytical solution of this problem is $\mathfrak{G}(x, t) = t^{3+\alpha} \sin(\pi x)$. The approximate solution and AEs with $k = \tilde{k} = 1, M =$

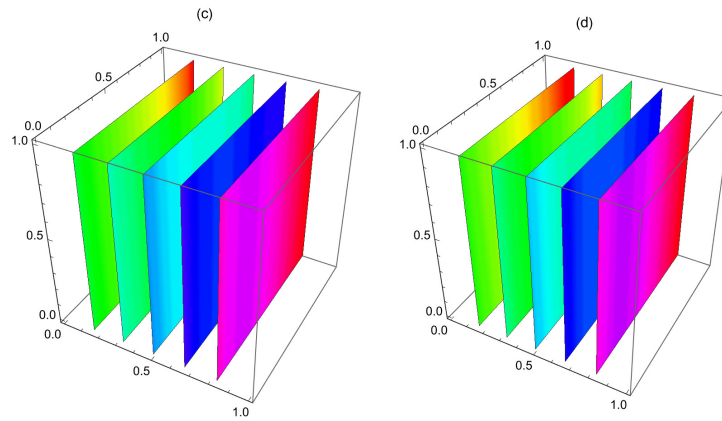


Figure 6: The density of (c) exact solution and (d) approximate solution with $k = 1, \tilde{k} = 2, M = 10, \tilde{M} = 6$, and $\alpha = 1$ in Sample 2.

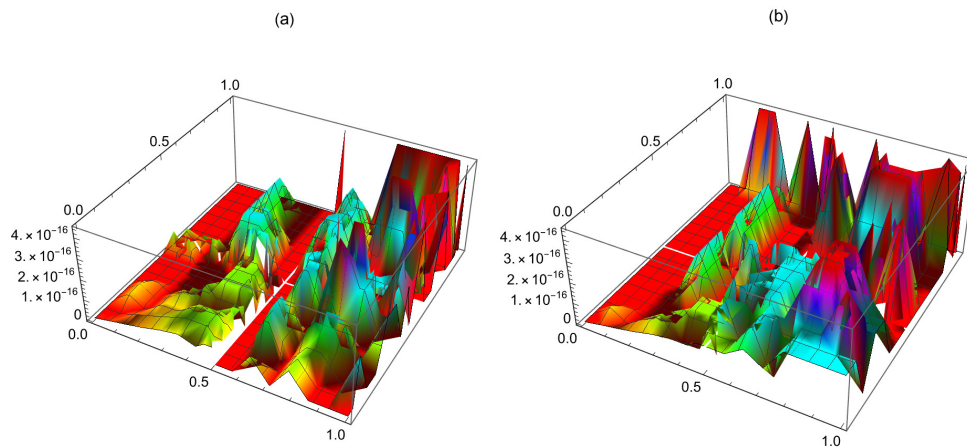


Figure 7: AEs with $k = \tilde{k} = 2, M = \tilde{M} = 2$, (a) $\alpha = 0.5$ and (b) $\alpha = 0.3$ in Sample 3.

8, $\tilde{M} = 5$, for $\alpha = 1$ is plotted in Figure 8. Moreover, a comparison of the exact solution with the approximate solution for some values of α , with $k = 1, \tilde{k} = 2, M = \tilde{M} = 5$ at $t = 0.5$ are shown in Figure 9. In $\alpha = 0.6$, the maximum error of the numerical solution derived by the present technique ($k = 1, \tilde{k} = 2, M = \tilde{M} = 5$) and finite difference method [50] are listed in Table 3.

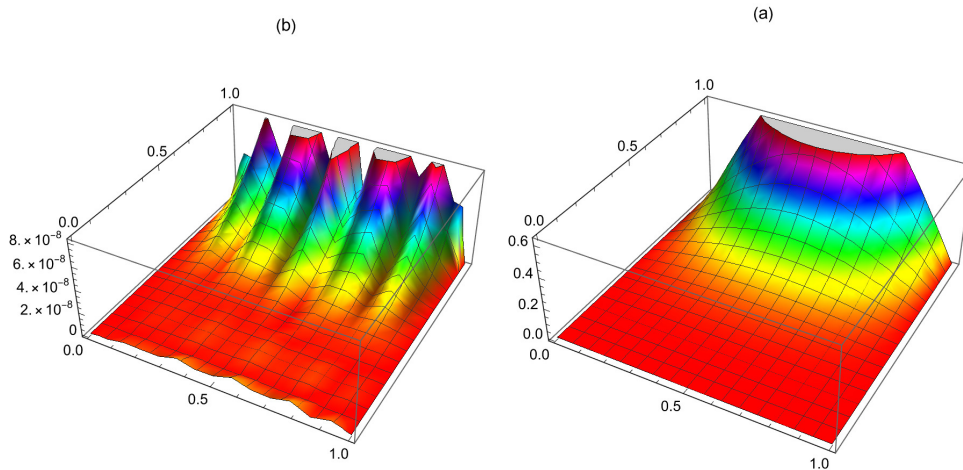


Figure 8: (a) The approximate solution and (b) AEs with $k = \tilde{k} = 1, M = 8, \tilde{M} = 5$, for $\alpha = 1$ in Sample 4.

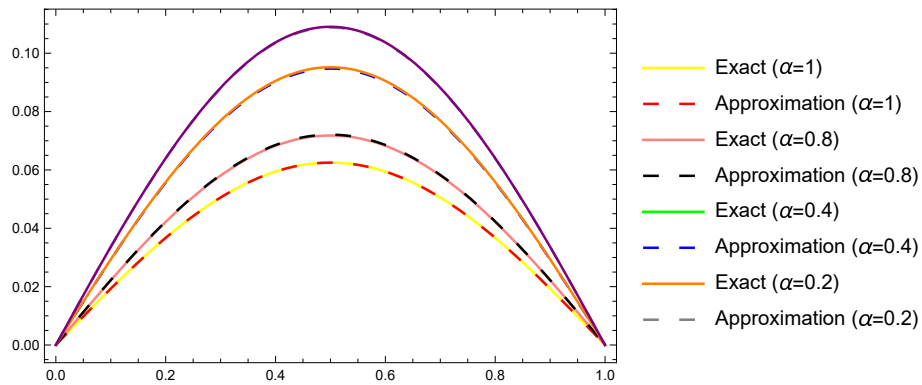


Figure 9: Comparison of the exact solution with the approximate solution for some values of α , with $k = 1, \tilde{k} = 2, M = \tilde{M} = 5$ at $t = 0.5$, in Sample 4.

7 Conclusion

This manuscript focused on suggesting an optimization technique to solve time-fractional convection-diffusion equations. Our aim was achieved by converting the considered problem to time-fractional partial integro-differential equations using the properties of Riemann-Liouville fractional integration. This process was used to improve the accuracy of the developed method. To develop the method, we used the Pell wavelets. Then, a new fractional integration pseudo-operational matrix had been obtained. Next, by implementing of an optimization method, the converted problem is solved, numerically.

Despite utilizing a few terms of the Pell wavelets, the numerical results display the excellent behavior of the optimization scheme to obtain the approximate solution. Also, the figures and tables verified the effectiveness of the established method. As a future work, due to the advantage of the proposed method, we can combine this method with some potential numerical methods such as the least square, and the Ritz-Galerkin method to solve different kinds of frac-

Table 3: Comparison of the maximum errors obtained by the present and finite difference method for $\alpha = 0.8$ in Sample 4.

Methods	
Finite difference method ($M = 20, N = 20$)	$1.0563 e^{-2}$
Finite difference method ($M = 40, N = 40$)	$4.3954 e^{-3}$
Finite difference method ($M = 80, N = 80$)	$1.8610 e^{-3}$
Finite difference method ($M = 160, N = 160$)	$7.9719 e^{-4}$
Present method ($k = \tilde{k} = 1, M = 8, \tilde{M} = 5$)	$1.5000 e^{-4}$

tional differential problems arising in some mathematical models of phenomena in engineering, physics, and biology.

Conflicts of Interest. The authors declare that they have no conflicts of interest regarding the publication of this article.

Acknowledgments. The authors express their gratitude to the Editorial board and reviewers for their attention to our work and comments that allowed us to improve the quality of the work. This work has been supported by the Center for International Scientific Studies & Collaboration (CISSC), Ministry of Science Research and Technology.

References

- [1] P. Agarwal, D. Baleanu, Y. Chen, S. Momani and J. A. T. Machado, *Fractional Calculus*, In ICFDA: International Workshop on Advanced Theory and Applications of Fractional Calculus, Amman, 2018.
- [2] S. Salahshour, A. Ahmadian, N. Senu, D. Baleanu and P. Agarwal, On analytical solutions of the fractional differential equation with uncertainty: application to the basset problem, *Entropy* **17** (2015) 885–902, <https://doi.org/10.3390/e17020885>.
- [3] P. Agarwal and J. Choi, Fractional calculus operators and their image formulas, *J. Korean Math. Soc.* **53** (2016) 1183–1210, <https://doi.org/10.4134/JKMS.j150458>.
- [4] R. Akbari and L. Navaei, Fractional dynamics of infectious disease transmission with optimal control, *Math. Interdisc. Res.* **9** (2024) 199–213, <https://doi.org/10.22052/MIR.2023.253000.1410>.
- [5] M. Valizadeh, Y. Mahmoudi and F. Dastmalchi Saei, On fractional linear multi-step methods for fractional order multi-delay nonlinear pantograph equation, *Comput. Methods Differ. Equ.* **12** (2024) 511–522, <https://doi.org/10.22034/cmde.2023.58018.2444>.
- [6] M. Pourbabaee and A. Saadatmandi, A new operational matrix based on Müntz-Legendre polynomials for solving distributed order fractional differential equations, *Math. Comput. Simulation* **194** (2022) 210–235, <https://doi.org/10.1016/j.matcom.2021.11.023>.
- [7] M. Bisheh-Niasar, The effect of the Caputo fractional derivative on polynomiography, *Math. Interdisc. Res.* **8** (2023) 347–358, <https://doi.org/10.22052/MIR.2022.246736.1367>.

- [8] Z. Hammouch, T. Mekkaoui and P. Agarwal, Optical solitons for the Calogero-Bogoyavlenskii-Schiff equation in $(2 + 1)$ dimensions with time-fractional conformable derivative, *Eur. Phys. J. Plus* **133** (2018) 1–6, <https://doi.org/10.1140/epjp/i2018-12096-8>.
- [9] N. A. Shah, P. Agarwal, J. D. Chung, S. Althobaiti, S. Sayed, A. F. Aljohani and M. Alkafafy, Analysis of time-fractional Burgers and diffusion equations by using modified q-HATM, *Fractals* **30** (2022) #2240012, <https://doi.org/10.1142/S0218348X22400126>.
- [10] L. Shi, S. Rashid, S. Sultana, A. Khalid, P. Agarwal and M. S. Osman, Semi-analytical view of time-fractional PDES with proportional delays pertaining to index and Mittag-Leffler memory interacting with hybrid transforms, *Fractals* **31** (2023) #2340071, <https://doi.org/10.1142/S0218348X23400716>.
- [11] A. Saadatmandi, M. Dehghan and M. R. Azizi, The Sinc-Legendre collocation method for a class of fractional convection-diffusion equations with variable coefficients, *Commun. Nonlinear Sci. Numer. Simul.* **17** (2012) 4125–4136, <https://doi.org/10.1016/j.cnsns.2012.03.003>.
- [12] S. Sabermahani, Y. Ordokhani and S. A. Yousefi, Fractional-order general Lagrange scaling functions and their applications, *Bit Numer. Math.* **60** (2020) 101–128, <https://doi.org/10.1007/s10543-019-00769-0>.
- [13] A. S. Hendy and M. A. Zaky, A priori estimates to solutions of the time-fractional convection-diffusion-reaction equation coupled with the Darcy system, *Commun. Nonlinear Sci. Numer. Simul.* **109** (2022) #106288, <https://doi.org/10.1016/j.cnsns.2022.106288>.
- [14] L. Sun, X. Yan and T. Wei, Identification of time-dependent convection coefficient in a time-fractional diffusion equation, *J. Comput. Appl. Math.* **346** (2019) 505–517, <https://doi.org/10.1016/j.cam.2018.07.029>.
- [15] R. Kamal Kamran, G. Rahmat and K. Shah, On the numerical approximation of three-dimensional time fractional convection-diffusion equations, *Math. Probl. Eng.* **2021** (2021) #4640467, <https://doi.org/10.1155/2021/4640467>.
- [16] L. J. Chen, M. Li and Q. Xu, Sinc-galerkin method for solving the time fractional convection-diffusion equation with variable coefficients, *Adv. Differ. Equ.* **504** (2020) #504, <https://doi.org/10.1186/s13662-020-02959-5>.
- [17] A. Chang, H. Sun, C. Zheng, B. Lu, C. Lu, R. Ma, Y. Zhang, A time fractional convection-diffusion equation to model gas transport through heterogeneous soil and gas reservoirs, *Phys. A: Stat. Mech. Appl.* **502** (2018) 356–369, <https://doi.org/10.1016/j.physa.2018.02.080>.
- [18] M. R. S. Ammi and I. Jamiyai, Finite difference and Legendre spectral method for a time-fractional diffusion-convection equation for image restoration, *Discrete Contin. Dyn. Syst. Ser. S* **11** (2018) 103–117, <https://doi.org/10.3934/dcdss.2018007>.
- [19] X. Wang, D. Posny and J. Wang, A reaction-convection-diffusion model for cholera spatial dynamics, *Discrete Contin. Dyn. Syst. Ser. B* **21** (2016) 2785–2809, <https://doi.org/10.3934/dcdsb.2016073>.

- [20] S. Nagar, R. C. Korzekwa and K. Korzekwa, Continuous intestinal absorption model based on the convection-diffusion equation, *Mol. Pharm.* **14** (2017) 3069–3086, <https://doi.org/10.1021/acs.molpharmaceut.7b00286>.
- [21] M. P. D. Comşa, R. Phlypo and P. Grangeat, Inverting the diffusion-convection equation for gas desorption through an homogeneous membrane by Kalman filtering, *In 2022 30th European Signal Processing Conference (EUSIPCO)* 1318–1322 IEEE (2022).
- [22] M. Abbaszadeh, A. Bagheri Salec, S. Kamel and A. Al-Khafaji, The effect of fractional-order derivative for pattern formation of brusselator reaction–diffusion model occurring in chemical reactions, *Iranian J. Math. Chem.* **14** (2023) 243–269, <https://doi.org/10.22052/IJMC.2023.253498.1759>.
- [23] R. Hilfer, *Applications of Fractional Calculus in Physics*, World Scientific, Singapore, 2000.
- [24] I. M. Sokolov, J. Klafter and A. Blumen, Fractional kinetics, *Phys. Today.* **55** (2002) 48–54.
- [25] R. F. Sincovec and N. K. Madsen, Software for nonlinear partial differential equations, *ACM Trans. Math. Softw.* **1** (1975) 232–260.
- [26] X. Li and C. Xu, Existence and uniqueness of the weak solution of the space-time fractional diffusion equation and a spectral method approximation, *Commun. Comput. Phys.* **8** (2010) 1016–1051, <https://doi.org/10.4208/cicp.020709.221209a>.
- [27] L. Sun, X. Yan and T. Wei, Identification of time-dependent convection coefficient in a time-fractional diffusion equation, *J. Comput. Appl. Math.* **346** (2019) 505–517, <https://doi.org/10.1016/j.cam.2018.07.029>.
- [28] F. Liu, P. Zhuang, V. Anh, I. Turner and K. Burrage, Stability and convergence of the difference methods for the space-time fractional advection-diffusion equation, *Appl. Math. Comput.* **191** (2007) 12–20, <https://doi.org/10.1016/j.amc.2006.08.162>.
- [29] H. Safdari, Y. E. Aghdam and J. F. Gómez-Aguilar, Shifted Chebyshev collocation of the fourth kind with convergence analysis for the space-time fractional advection-diffusion equation, *Eng. Comput.* **38** (2022) 1409–1420, <https://doi.org/10.1007/s00366-020-01092-x>.
- [30] E. Sokhanvar, A. Askari-Hemmat and S. A. Yousefi, Legendre multiwavelet functions for numerical solution of multi-term time-space convection-diffusion equations of fractional order, *Eng. Comput.* **37** (2021) 1473–1484, <https://doi.org/10.1007/s00366-019-00896-w>.
- [31] A. Shirzadi, L. Ling and S. Abbasbandy, Meshless simulations of the two-dimensional fractional-time convection-diffusion-reaction equations, *Eng. Anal. Bound. Elem.* **36** (2012) 1522–1527, <https://doi.org/10.1016/j.enganabound.2012.05.005>.
- [32] M. M. Izadkhah and J. Saberi-Nadjafi, Gegenbauer spectral method for time-fractional convection-diffusion equations with variable coefficients, *Math. Methods Appl. Sci.* **38** (2015) 3183–3194, <https://doi.org/10.1002/mma.3289>.
- [33] M. Sh. Dahaghin and H. Hassani, A new optimization method for a class of time fractional convection-diffusion-wave equations with variable coefficients, *Eur. Phys. J. Plus* **132** (2017) 1–13, <https://doi.org/10.1140/epjp/i2017-11407-y>.

- [34] M. Behroozifar and A. Sazmand, An approximate solution based on Jacobi polynomials for time-fractional convection-diffusion equation, *Appl. Math. Comput.* **296** (2017) 1–17, <https://doi.org/10.1016/j.amc.2016.09.028>.
- [35] G. T. Lubo and G. F. Duressa, Linear B-spline finite element Method for solving delay reaction diffusion equation, *Comput. Methods Differ. Equ.* **11** (2023) 161–174, <https://doi.org/10.22034/CMDE.2022.49678.2066>.
- [36] E. Keshavarz, Y. Ordokhani and M. Razzaghi, A numerical solution for fractional optimal control problems via Bernoulli polynomials, *J. Vib. Control* **22** (2016) 3889–3903, <https://doi.org/10.1177/1077546314567181>.
- [37] S. Sabermahani and Y. Ordokhani, Fibonacci wavelets and Galerkin method to investigate fractional optimal control problems with bibliometric analysis, *J. Vib. Control* **27** (2021) 1778–1792, <https://doi.org/10.1177/1077546320948346>.
- [38] F. Nourian, M. Lakestani, S. Sabermahani and Y. Ordokhani, Touchard wavelet technique for solving time-fractional Black-Scholes model, *Comp. Appl. Math.* **41** (2022) 3150, <https://doi.org/10.1007/s40314-022-01853-y>.
- [39] P. T. Toan, T. N. Vo and M. Razzaghi, Taylor wavelet method for fractional delay differential equations, *Eng. Comput.* **37** (2021) 231–240, <https://doi.org/10.1007/s00366-019-00818-w>.
- [40] Y. Taşyurdu, D. Çifçi and Ö. Deveci, Applications of Pell polynomials in rings, *J. Math. Res.* **10** (2018) 35–41, <https://doi.org/10.5539/jmr.v10n3p35>.
- [41] M. Taghipour and H. Aminikhah, A fast collocation method for solving the weakly singular fractional integro-differential equation. Computational and Applied Mathematics, *Comp. Appl. Math.* **41** (2022) 1–38, <https://doi.org/10.1007/s40314-022-01845-y>.
- [42] P. F. Byrd, Expansion of analytic functions in polynomials associated with Fibonacci numbers, *Fibonacci Quart.* **1** (1963) 16–29.
- [43] S. Sabermahani, Y. Ordokhani and M. Razzaghi, Ritz-generalized Pell wavelet method: Application for two classes of fractional pantograph problems, *Commun. Nonlinear Sci. Numer. Simul.* **119** (2023) #107138, <https://doi.org/10.1016/j.cnsns.2023.107138>.
- [44] S. Mashayekhi and M. Razzaghi, Numerical solution of distributed order fractional differential equations by hybrid functions, *J. Comput. Phys.* **315** (2016) 169–181, <https://doi.org/10.1016/j.jcp.2016.01.041>.
- [45] S. Sabermahani, Y. Ordokhani and S. A. Yousefi, Fibonacci wavelets and their applications for solving two classes of time-varying delay problems, *Optimal Control Appl. Methods* **41** (2020) 395–416, <https://doi.org/10.1002/oca.2549>.
- [46] C. Canuto, M. Y. Hussaini, A. Quarteroni and T. A. Zang, *Spectral Methods: Fundamentals in Single Domains*, Springer-Verlag Berlin Heidelberg, 2006.
- [47] H. Dehestani, Y. Ordokhani and M. Razzaghi, On the applicability of Genocchi wavelet method for different kinds of fractional-order differential equations with delay, *Numer. Linear Algebra Appl.* **26** (2019) #e2259, <https://doi.org/10.1002/nla.2259>.

- [48] F. Zhou and X. Xu, The third kind Chebyshev wavelets collocation method for solving the time-fractional convection diffusion equations with variable coefficients, *Appl. Math. Comput.* **280** (2016) 11–29, <https://doi.org/10.1016/j.amc.2016.01.029>.
- [49] Y. Chen, Y. Wu, Y. Cui, Z. Wang and D. Jin, Wavelet method for a class of fractional convection-diffusion equation with variable coefficients. *J. Comput. Sci.*, **1** (2010) 146–149, <https://doi.org/10.1016/j.jocs.2010.07.001>.
- [50] J. Zhang, X. Zhang and B. Yang, An approximation scheme for the time fractional convection-diffusion equation, *Appl. Math. Comput.* **335** (2018) 305–312, <https://doi.org/10.1016/j.amc.2018.04.019>.